An experiment to measure the recombination rate of oxygen

By J. WILSON*

Graduate School of Aeronautical Engineering, Cornell University, Ithaca, New York

(Received 22 October 1962)

The feasibility of an experiment to measure the recombination rate of oxygen is examined using the ideal-dissociating-gas model. The experiment is to be performed in a shock tube, the shock-heated (and dissociated) gas being cooled by passing it through a Prandtl–Meyer expansion, and then allowed to recombine in a constant-area channel. At appropriate densities and shock Mach numbers it is found that recombination takes place in a distance suitable for a laboratory experiment.

Using this technique, the recombination rate of oxygen has been measured at 2700 °K. To determine the recombination rate, the absorption of ultraviolet light at a wavelength of 2283 Å measured 11 cm downstream of the expansion was compared with absorptions calculated for various values of the recombination rate constant.

The measured value of the recombination rate constant of oxygen is in agreement with values calculated from dissociation rate measurements.

1. Introduction

Current estimates of recombination rates are usually derived from dissociation rate measurements by dividing the dissociation rate constant by the equilibrium constant. Thus, for the oxygen dissociation reaction

$$O_2 + M = 2O + M, \tag{1}$$

in which M is some third body, the rate of the reaction is expressed as

$$d[O_2]/dt = k_R[O]^2\,[M] - k_D[O_2]\,[M] \tag{2}$$

in which k_R and k_D are the recombination and dissociation rate constants respectively, so that at equilibrium, when the rate of the reaction must be zero,

$$\frac{k_D}{k_R} = \frac{[O]^2_{\text{eq.}}}{[O_2]_{\text{eq.}}} = K. \tag{3}$$

K, the equilibrium constant, is known from statistical mechanics. However, equation (3), relating the dissociation and recombination rate constants, is strictly true only at equilibrium, and in fact rate constants are always measured away from equilibrium so that their use in equation (3) is not immediately justi-

---

* Now at Royal Aircraft Establishment, Farnborough, Hampshire, England.

fiable. Since several measurements of the dissociation rate of oxygen (Anderson 1961; Byron 1959; Camac & Vaughan 1959; Matthews 1959; Rink, Knight & Duff 1961; Schexnayder & Evans 1961) have already been made, the validity of using non-equilibrium rate constants in equation (3) could be checked if the recombination rate of oxygen were measured directly. Some such measurements (Golden & Myerson 1958; Kretschmer & Peterson 1960; Reeves, Manella & Harteck 1960) have been performed at, or near, room temperature, which is outside the temperature range of the dissociation rate measurements. The work reported here is a measurement of the recombination rate of oxygen around 2700 °K.

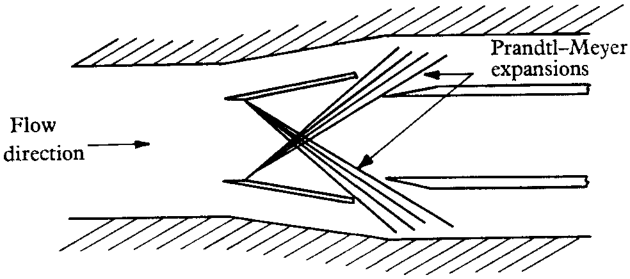

FIGURE 2. Diagram of flow in test-section

The measurement of the recombination rate was undertaken also in the hope that it would determine the temperature dependence of the rate constants more accurately than would a measurement of the dissociation rate. In principle this should be possible since collision theory indicates that the recombination rate constant is proportional to a power of the temperature only, whereas the dissociation rate constant is proportional to the product of a power of the temperature and $\exp(-T_D/T)$, of which the temperature dependence is dominated by the exponential. (T_D is the dissociation energy expressed as a temperature.) In practice, the temperature range covered by the experiment was too small to determine the temperature dependence.

2. Designing the experiment

In an experiment to measure the recombination rate, the oxygen must first be dissociated and then allowed to recombine. Dissociation can be achieved by heating the gas using a shock wave generated in a shock tube (Anderson 1961; Byron 1959; Camac & Vaughan 1959; Matthews 1959; Rink *et al.* 1961; Schexnayder & Evans 1961). In order to make the gas recombine, it must then be cooled. It was considered that letting the dissociated gas behind the shock flow through a Prandtl-Meyer expansion was the most convenient method of cooling the gas (though by no means the only method). The arrangement used to generate the expansion is shown in figure 1, plate 1, and drawn schematically in figure 2. Two aerofoils, one mounted on the top, and one on the bottom of the tube, expand the flow, which then streams into a constant-area channel. If the experimental conditions have been chosen correctly, the time taken by the flow to cross the expansion fan will be much shorter than the recombination time. The flow will therefore be frozen on entering the constant-area channel, and recombination will take place as the gas flows along the channel.

In order to determine if such an experiment is feasible on a laboratory scale, and if so, what the appropriate experimental conditions are, the flow of an ideal dissociating gas through the geometry of the experiment will be calculated. The concept of an ideal dissociating gas was introduced by Lighthill (1957). When undissociated, this is a diatomic gas with constant specific heats for which the vibrational mode is considered as half excited, giving the molecule six degrees of freedom. If this diatomic gas is mixed with a monatomic gas such that c is the initial ratio of the number of diatomic particles per unit volume to the total number, the enthalpy H for the mixture is

$$H = [\tfrac{5}{2}+c(\tfrac{3}{2}+\alpha)]\,(R/m)\,T+\alpha c(R/m)\,T_D, \tag{4}$$

where m is the average molecular weight of the gas mixture, given by

$$m_{\text{monatomic}}(1-c)+cm_{\text{diatomic}};$$

T is temperature, T_D the dissociation energy expressed as a temperature, and R the universal gas constant. The gas law for the mixture is

$$p = \rho(1+c\alpha)\,(R/m)\,T, \tag{5}$$

where p is pressure, ρ is density, and α the degree of dissociation.

In the experiment, the gas is first dissociated by a shock wave, then flows through the Prandtl–Meyer expansion without change in the degree of dissociation, and finally recombines in the constant-area channel. Consequently, the first step is to calculate the conditions behind a shock wave propagating into a mixture of an ideal dissociating gas and a monatomic gas.

2.1. *Conditions behind the shock wave*

It will be assumed that equilibrium conditions hold behind the shock. This will be the case if the dissociation time is short. For the temperatures and densities used in the experiment, equilibrium was attained within about 10 μsec (see Byron 1959) and measurements were always made later than 20 μsec after the shock passage. At equilibrium the law of mass action for the gas mixture gives

$$\frac{\alpha^2}{1-\alpha} = \frac{\rho_D}{c\rho}\exp\left(-T_D/T\right), \tag{6}$$

where ρ_D is a constant with the dimensions of density. This equation must be solved simultaneously with the usual conservation equations and the equation of state. Since an approximate solution is all that is required to design the experiment, the strong-shock form of these equations may be used; in shock-fixed co-ordinates these are:

conservation of mass $\quad \rho_0 u_0 = \rho_1 u_1;$ (7)

conservation of momentum $\quad \rho_0 u_0^2 = p_1+\rho_1 u_1^2;$ (8)

conservation of energy $\quad \tfrac{1}{2}u_0^2 = H_1,$ (9)

where the suffix 0 denotes conditions ahead of the shock and the suffix 1 denotes conditions behind it; u denotes velocity as seen in shock-fixed co-ordinates; q will be used later for velocity as seen in laboratory co-ordinates.

Using the equation of state and the definition of enthalpy, these equations combine to give

$$\frac{\rho_1}{\rho_0} = \frac{2H_1}{(1+c\alpha_1)(R/m)T_1} - 1. \tag{10}$$

Eliminating ρ_1 with the equilibrium equation gives

$$(1+c\alpha_1)(1-\alpha_1)\rho_D \exp(-T_D/T_1) = c\rho_0\alpha_1^2[4+c(3+\alpha_1)+2c\alpha_1 T_D/T_1]. \tag{11}$$

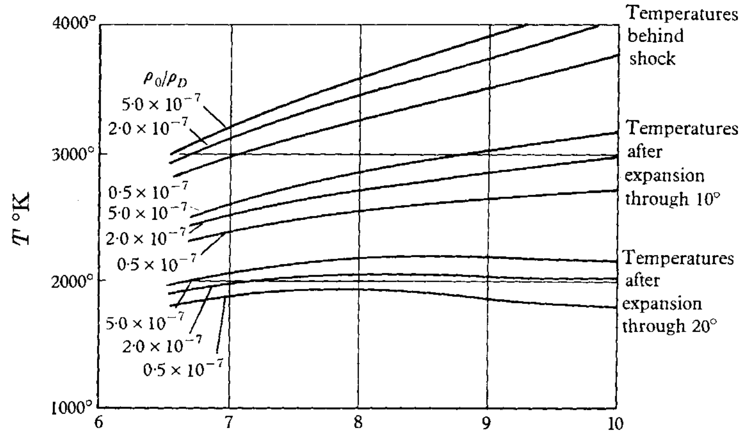

FIGURE 3. Temperatures behind the shock, and after expansion, against shock Mach number for a 30 % mixture of an ideal dissociating gas in a monatomic gas.

This is a cubic equation which, given T_1, can be solved for α_1, with ρ_0 as a parameter. The Mach number of the shock, M_0, is then given by

$$M_0 = \frac{u_0}{a_0} = \left[2H_1 \Big/ \frac{5+3c}{3(1+c)}\frac{R}{m}T_0\right]^{\frac{1}{2}} = \left[\{[5+2c(\tfrac{3}{2}+\alpha_1)]\,T_1 + 2\alpha c T_D\} \Big/ \frac{5+3c}{3(1+c)}T_0\right]^{\frac{1}{2}}, \tag{12}$$

where a_0 is the undissociated speed of sound, which will be applicable in front of the shock.

Values of the dissociation constants appropriate for oxygen are $\rho_D = 170\,\text{g/c.c.}$ and $T_D = 60{,}000\,°\text{K}$. Using these values, and $T_0 = 300\,°\text{K}$, the conditions behind strong shocks in a 30 % mixture of an ideal dissociating gas with a monatomic gas have been found, and are given in figures 3 to 6.

2.2. *Flow through a Prandtl–Meyer expansion*

The conditions behind the shock wave give the state of the gas entering the Prandtl–Meyer expansion. The change across the expansion is now required. If recombination is frozen, i.e. $\alpha = \alpha_1$, throughout the expansion, the specific heats of the gas are constant, and their ratio is given by

$$\gamma = \frac{dH}{dE} = \frac{5+c(3+2c\alpha_1)}{3(1+c)}. \tag{13}$$

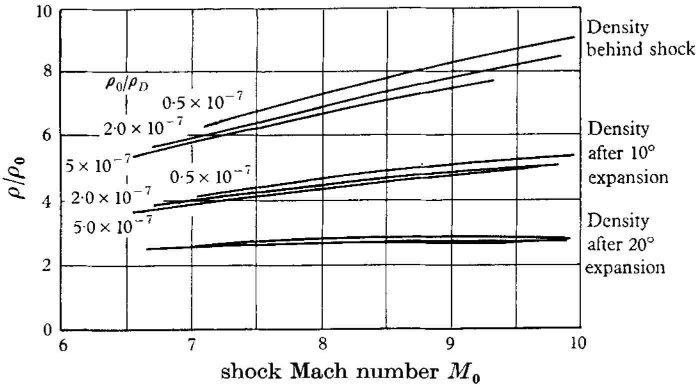

FIGURE 4. Densities behind the shock, and after expansion, against shock Mach number for a 30 % mixture of an ideal dissociating gas in a monatomic gas.

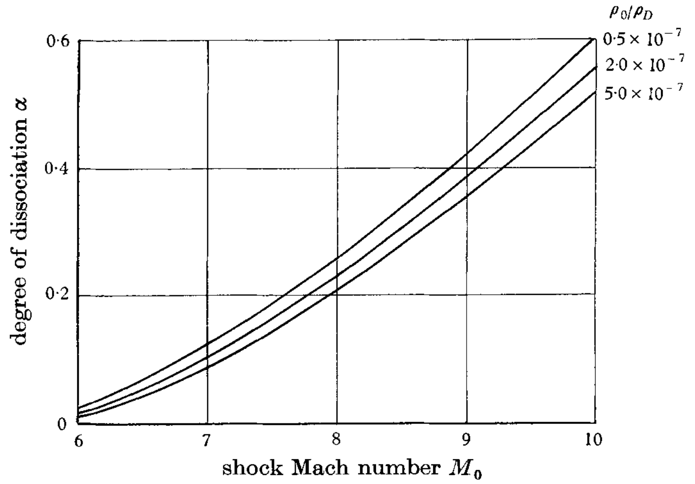

FIGURE 5. Degree of dissociation behind shock waves in a 30 % mixture of an ideal dissociating gas in a monatomic gas.

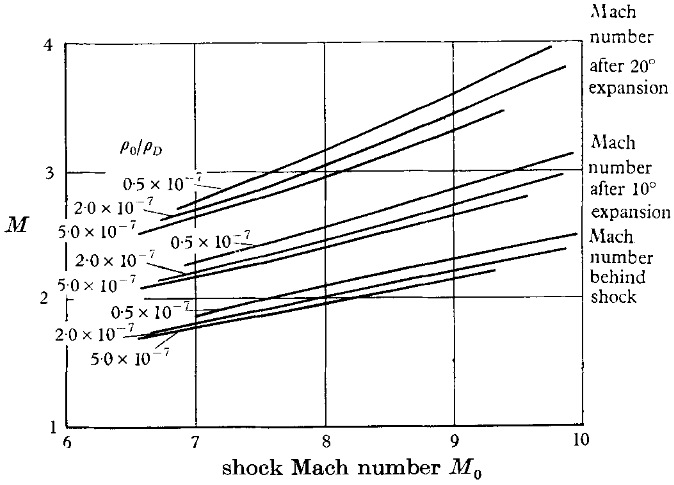

FIGURE 6. Mach number of the flow behind the shock, and after expansion against shock Mach number for a 30 % mixture of an ideal dissociating gas in a monatomic gas.

The assumption that recombination is frozen requires justification. It will be valid if the time of the flow through the expansion is short compared with the time required to recombine. The experimental conditions will be chosen to make this true.

The property angle for a gas with the specific heat ratio given above is

$$\nu = \left\{\frac{4+c(3+\alpha_1)}{(1+c\alpha_1)}\right\}^{\frac{1}{2}} \tan^{-1}\left\{\frac{(1+c\alpha_1)}{4+c(3+\alpha_1)}(M^2-1)\right\}^{\frac{1}{2}} - \tan^{-1}(M^2-1)^{\frac{1}{2}}. \tag{14}$$

This equation is used in the usual way (N.A.C.A. Report 1135, p. 14) to obtain the change of Mach number across the expansion. The curves of property angle versus Mach number for various degrees of dissociation are given in figure 7. The Mach number entering the expansion is, of course, determined by the Mach number behind the shock as seen in laboratory co-ordinates, i.e.

$$M_1 = q_1/a_1 = (u_0 - u_1)/a_1. \tag{15}$$

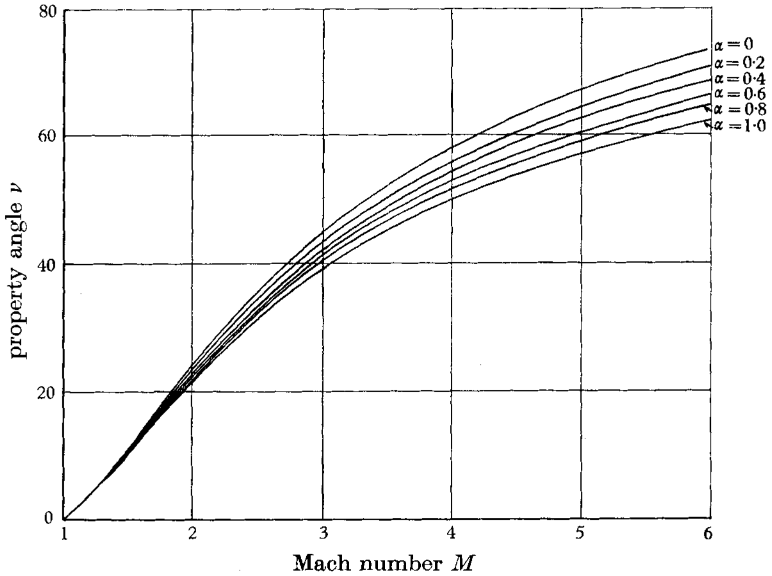

FIGURE 7. Property angle against Mach number for various values of the degree of dissociation for a 30 % mixture of an ideal dissociating gas in a monatomic gas.

The Mach number M_2 after expansion through angles of 10° and 20° is plotted in figure 6. The suffix 2 is used to denote conditions immediately behind the expansion.

The energy equation can be written to give the temperature ratio across the expansion

$$\frac{T_2}{T_1} = \left\{1 + M_1^2\frac{(1+c\alpha_1)}{3(1+c)}\right\} \bigg/ \left\{1 + M_2^2\frac{(1+c\alpha_1)}{3(1+c)}\right\}, \tag{16}$$

and the density ratio follows since for a gas with constant specific heats

$$\rho_2/\rho_1 = (T_2/T_1)^{1/\gamma-1} \tag{17}$$

so that in the present case

$$\rho_2/\rho_1 = (T_2/T_1)^{3(1+c)/2(1+c\alpha_1)}. \tag{18}$$

The temperatures and densities behind the Prandtl–Meyer expansions of the flow following the shock waves of § 2.1 are plotted in figures 3 and 4.

2.3. *Recombination behind the expansion*

After leaving the expansion, the gas flows into a constant-area channel, where recombination takes place. Thus the one-dimensional conservation equations apply. Using the gas law to eliminate the pressure from the equation of conservation of momentum, and using the equation of conservation of energy to eliminate the velocity, gives

$$T = \frac{1}{[2+c(\frac{3}{2}+\frac{1}{2}\alpha)]\,(R/m)}\left[H_2+\tfrac{1}{2}q_2^2-\alpha c\frac{R}{m}T_D-\frac{p_2+\rho_2 q_2^2}{2\rho}\right]. \tag{19}$$

Substituting the gas law and conservation of mass into the momentum equation, eliminating the temperature with the energy equation, and using the definition of enthalpy leads to

$$\begin{aligned}\frac{1}{\rho} = {}& \frac{(p_2+\rho_2 q_2^2)}{2(\rho_2 q_2)^2}\left(\frac{\frac{5}{2}+c(\frac{3}{2}+\alpha)}{2+c(\frac{3}{2}+\frac{1}{2}\alpha)}\right)\\ &\times\left\{1+\left(1-\frac{4(\rho_2 q_2)^2\,(1+c\alpha)\,(2+c[\frac{3}{2}+\frac{1}{2}\alpha])}{(p_2+\rho_2 q_2^2)^2\,(\frac{5}{2}+c[\frac{3}{2}+\alpha])^2}\left[H_2+\tfrac{1}{2}q_2^2-\alpha c\frac{R}{m}T_D\right]\right)^{\frac{1}{2}}\right\}. \end{aligned} \tag{20}$$

One more equation is required to specify the flow. This is the equation determining the rate of the chemical reaction. If a simple Arrhenius form for the dissociation rate constant is used, i.e.

$$k_D = c_D \exp(-T_D/T), \tag{21}$$

the rate equation becomes

$$\rho(d\alpha/dx) = c_D\rho^2[(1-\alpha)\exp(-T_D/T)-c\alpha^2\rho/\rho_D]. \tag{22}$$

This expression, which effectively assumes that all third bodies have equal efficiency, is a simplified form of that used by Freeman (1957). In laboratory-fixed co-ordinates

$$d\alpha/dt = q(d\alpha/dx), \tag{23}$$

where x is distance measured along the constant-area channel from the expansion. Equations (22) and (23) combine with the equation of conservation of mass

$$\rho_2 q_2 = \rho q \tag{24}$$

to give

$$x = \rho_2 q_2 \int_{\alpha_2}^{\alpha} \frac{d\alpha}{c_D\rho^2\,[(1-\alpha)\exp(-T_D/T)-c\alpha^2\rho/\rho_D]}. \tag{25}$$

Since ρ and T are known as functions of α from equations (19) and (20), the integration can be performed, thereby determining α, and hence ρ and T, as a function of x. The calculation has been done for three values of shock Mach number for expansions through 10° and 20°. The results are shown in figures 8, 9 and 10. For this calculation c_D has been taken equal to $5\times10^{14}\,\mathrm{cm^3\,g^{-1}\,sec^{-1}}$, which is approximately the value for oxygen, and $R/m = 3\times10^6\,\mathrm{erg/g\,^\circ K}$.

The calculation showed that during recombination the density remained constant to within 3 %, so it is not a sensitive measure of the degree of the reaction. However, because of the dependence of the recombination rate on the cube of the density, the value of the density strongly affects the recombination

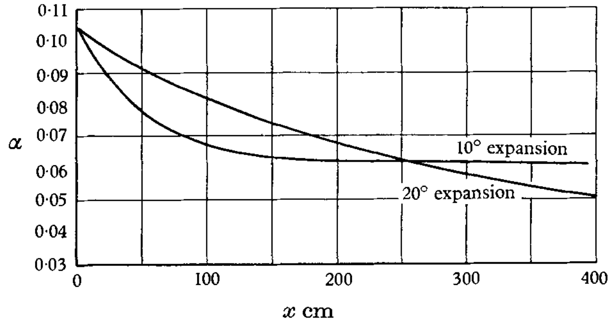

FIGURE 8. Recombination downstream of the expansion for a shock Mach number of 7, $\rho_0/\rho_D = 2{\cdot}0 \times 10^{-7}$.

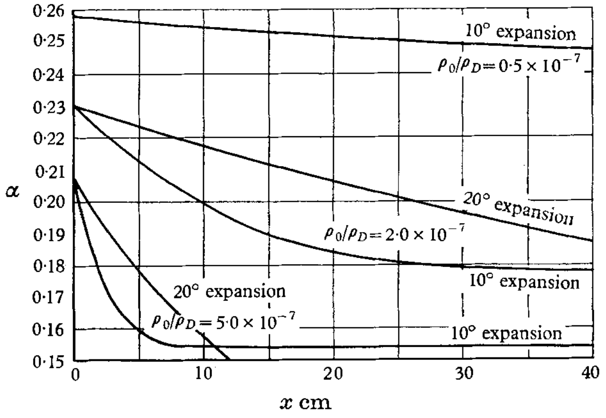

FIGURE 9. Recombination downstream of the expansion for a shock Mach number of 8.

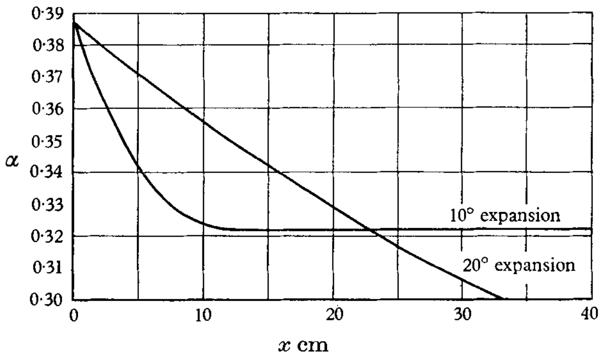

FIGURE 10. Recombination downstream of the expansion for a shock Mach number of 9, $\rho_0/\rho_D = 2{\cdot}0 \times 10^{-7}$.

distance. Thus expansion through the larger angle, and therefore to a lower density, results in a longer recombination distance. For a given initial density and expansion angle, a higher shock Mach number causes faster recombination because of the greater density ratio across the shock. With an expansion angle of 10°, and an initial density of $3{\cdot}4 \times 10^{-5}$ g/c.c. the recombination distance is of the order of 20 cm at Mach 8. This is short enough to be practical, and yet long enough to make valid the assumption that recombination is frozen through the expansion, as the expansion can be designed to take only a few centimetres. Consequently, a 10° expansion, and an initial density of about $3{\cdot}4 \times 10^{-5}$ g/c.c. were chosen for the experiment.

3. Preliminary experiments

Prior to the experiment itself, two preliminary experiments were run in order to check the density ratio across a Prandtl–Meyer expansion of dissociated gas, and to check the alignment of the apparatus, respectively.

(*a*) *Measurement of the density ratio across an expansion*

The measurement of the density ratio across an expansion was performed in the Graduate School of Aeronautical Engineering $1\frac{1}{2}$ in. shock tube (Byron 1959). This tube is equipped with a Mach–Zehnder interferometer, of which both beams pass through the tube. The model shown in figure 11, plate 1, was put into the tube so that the model appeared in the upstream window; the downstream window was not obstructed by the support. The top of the model was parallel to the incident flow for a length of 6 mm, then inclined at 10° away from it. Underneath the model was inclined 12° to the incident flow, this being approximately the maximum angle which allowed an attached shock for the conditions of the experiment.

Two spark light sources for the interferometer were used. Both were triggered by the amplified signal from a heat-transfer gauge situated 8 in. upstream of the first window, one a xenon spark of 200 μsec, duration, directly, and the other a 1 μsec duration air spark, via a delay circuit. The delay was such that the spark fired after the shock has passed the window, so that, by placing an interference filter in the light beam, a monochromatic picture of the flow over the model was obtained. Light from the xenon spark passed underneath the model, and then fell on a slit focused on a drum camera. The interferometer was adjusted to give white light fringes, which jumped when the shock crossed the effective position of the slit in the first window. Thus the time between the onset of the spark and the jump of the fringes was a measure of the shock speed. (Delay in initiation of the spark was calibrated using a photomultiplier.) Figure 12, plate 2, is a picture obtained in these tests. It will be noticed that there is a disturbance coming from the leading edge of the model, despite its being ground to a very fine edge. Indeed, Lighthill (1955) has suggested that such a disturbance is unavoidable. It is, however, a very weak disturbance and does not affect the density.

Shocks at Mach numbers between 8·5 and 10·5 were run into 50 % mixtures of oxygen and argon at a pressure of 2 cm Hg. The driver gas was heated to obtain the higher Mach numbers. The density behind the expansion calculated from the fringe displacement is given in figure 13 and compared with theory. The experimental error (which is determined by the accuracy to which the fringe jump can be measured) is too great to discriminate unequivocally between the frozen and equilibrium cases. However, the difference between the two cases is very small, and the object of the experiment was rather to check that the use of the frozen recombination calculations would give the correct value of the density. This it can be said to do.

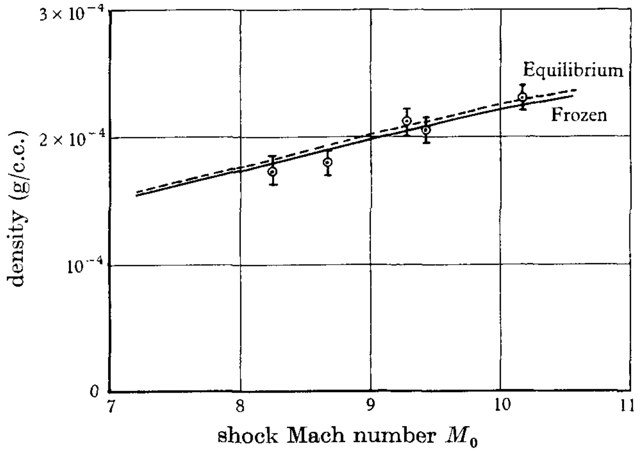

FIGURE 13. Theoretical and experimental values of density behind 10° expansions. Test gas is 50 % argon 50 % oxygen at 2 cm Hg pressure.

(b) Alignment of the apparatus

The experiment itself was carried out in a 1·8 in. square shock tube (described more fully by Wilson 1962*a*, *b*) to which was attached the working section of figure 1, plate 1. In order to verify that the flow through the aerofoils was as indicated in figure 2, schlieren pictures of the flow were taken. Figure 14, plate 1, is one of these photographs. It will be seen that the flow is as predicted except for the leading-edge disturbance which consists of a compression wave followed by an expansion, as suggested by Lighthill (1955). It was assumed, however, that the disturbance was weak, as in the previous experiment.

4. Description of the experiment

Apart from the working section (figure 1) the shock tube was a conventional 1·8 in. square tube. Before a run it was pumped down to a pressure of about 1 μ of mercury, and the leak rate was always less than 2 μ per minute. The test gas was a mixture of oxygen and argon which had been allowed to mix for at least one day in a mixing chamber. The oxygen and argon were Linde MSC grade having impurity levels of 36 and 10 p.p.m., respectively.

A schematic drawing of the apparatus is given in figure 15. Two measurements were made in the experiment, namely, shock speed and a measurement of the state of the gas downstream of the expansion by ultraviolet absorption. The shock speed was measured with silicon-dioxide-coated heat-transfer gauges. The signals from the gauges were differentiated and displayed on one beam of a Tektronix 555 oscilloscope via a differential plug-in unit (thereby cancelling out any noise present).

The source of ultraviolet light for the absorption measurement was a 'homemade' flash tube. Light from this source was made parallel by a quartz lens, and after passing through the shock tube 11 cm downstream of the expansion, was focused on the slit of a Seya–Namioka monochromator. The light intensity at the exit slit was monitored by an E.M.I. 6255*B* photomultiplier, the signal being fed to the other beam of the oscilloscope. The monochromator was set at 2283 Å, with a band pass of 16 Å. A Baird-Atomic ultraviolet interference filter (centred at 2280 Å) was placed before the entrance to the monochromator to cut out scattered light in the signal.

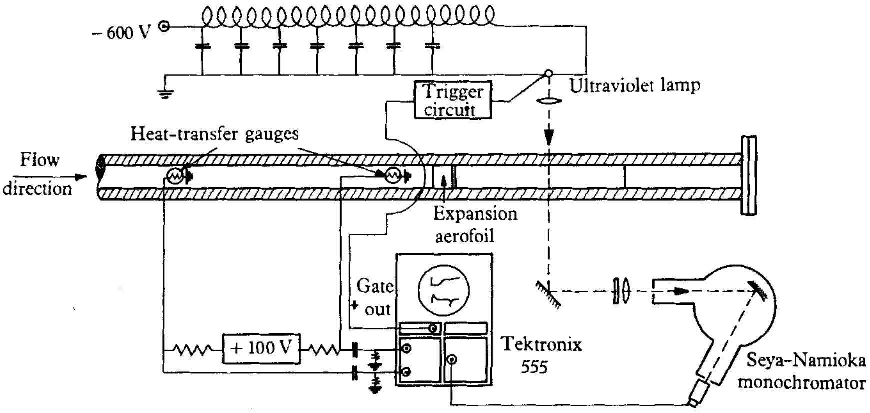

FIGURE 15. Schematic drawing of apparatus.

It was hoped that by using a transmission line to provide the energy for the spark, a square-wave light-pulse would be achieved. Whilst this was possible in the visible, it did not prove so in the ultraviolet, for some reason connected with electrode melting. Accordingly, a lamp was designed with hollow electrodes made of Elkonite (machineable tungsten manufactured by Mallory Metals, Inc.) to minimise electrode melting. In use, the lamp was filled with hydrogen to a pressure of about 2 mm of mercury, and the transmission line was charged to 600 V. The spark was fired by a 5 kV pulse from a thyratron trigger circuit, which was applied to a piece of wire wrapped round the quartz tube. The ultraviolet output of the lamp is shown in figure 16(*a*) marked 'reference trace'.

Figure 16(*a*) is an oscillogram taken during a run, and the transmission measured from it is given in figure 16(*b*). Until the shock arrives, the transmission is unity; following the shock there are two periods of approximately constant transmission, before the arrival of the interface. The experimental arrangement is essentially a straight-through shock tunnel, and therefore the starting process consists of a transmitted and a starting shock (see, e.g. figure 3.2(*b*) of Ferri 1961). The first period of constant transmission corresponds to the region between these shocks; it is the second period of constant transmission that constitutes the measurement.

The chief source of experimental error was the use of two spark flashes to determine the transmission—one during the run, and one afterwards to provide the reference trace. The light intensity was usually reproducible to within 3 %. This error could be eliminated entirely by using a second monochromator to view the spark directly during the run, thereby obtaining the incident and transmitted intensities for the same flash.

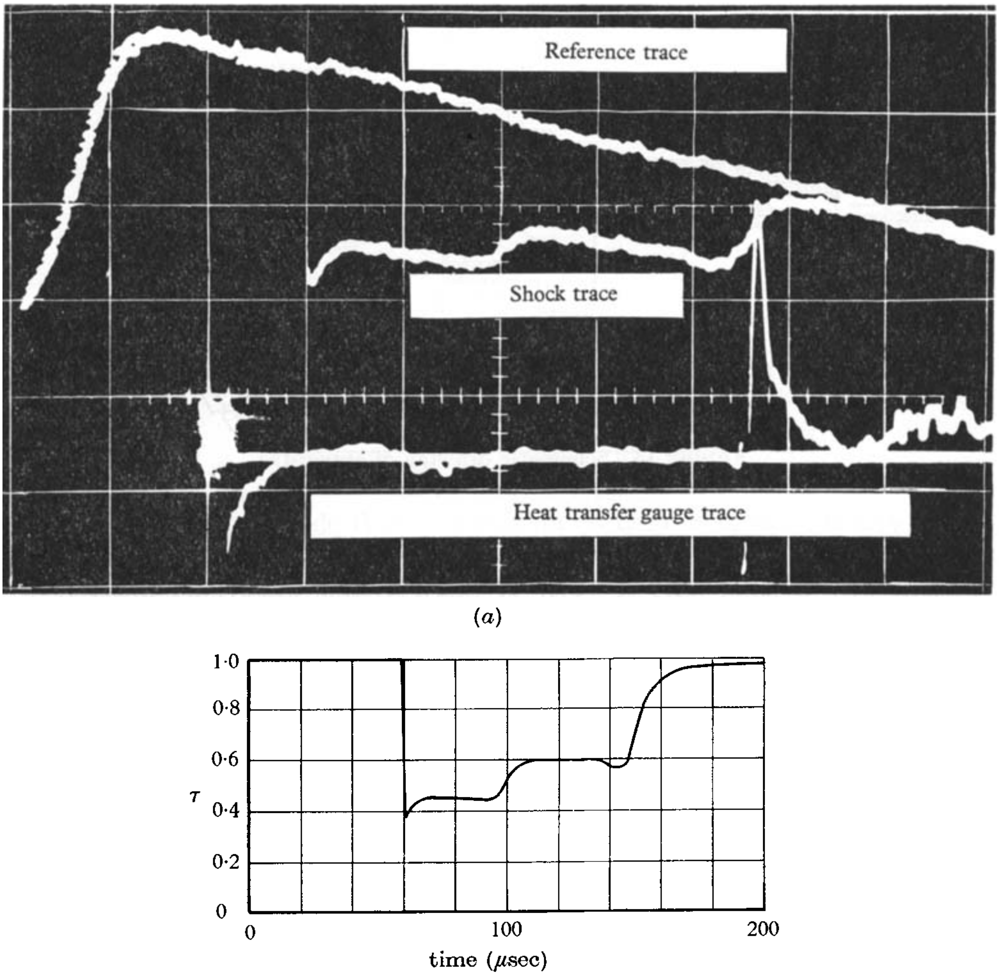

(a)

(b)

FIGURE 16 (a). Oscillogram of run at Mach 8·64. (b) Transmission measured from oscillogram.

5. The absorption technique

The possibility of using ultraviolet absorption to measure the state of oxygen has been suggested by Wurster & Treanor (1959), who measured the absorption behind shocks in oxygen in each of four channels about 20 Å wide, between 2280 and 2870 Å. The transitions involved are from excited vibrational-rotational states, and since the absorption coefficient is proportional to the population of these states, it is both temperature and density dependent. The average transmission for broad-band absorption is given by

$$\bar{\tau} = \exp(-\bar{K}NL), \tag{26}$$

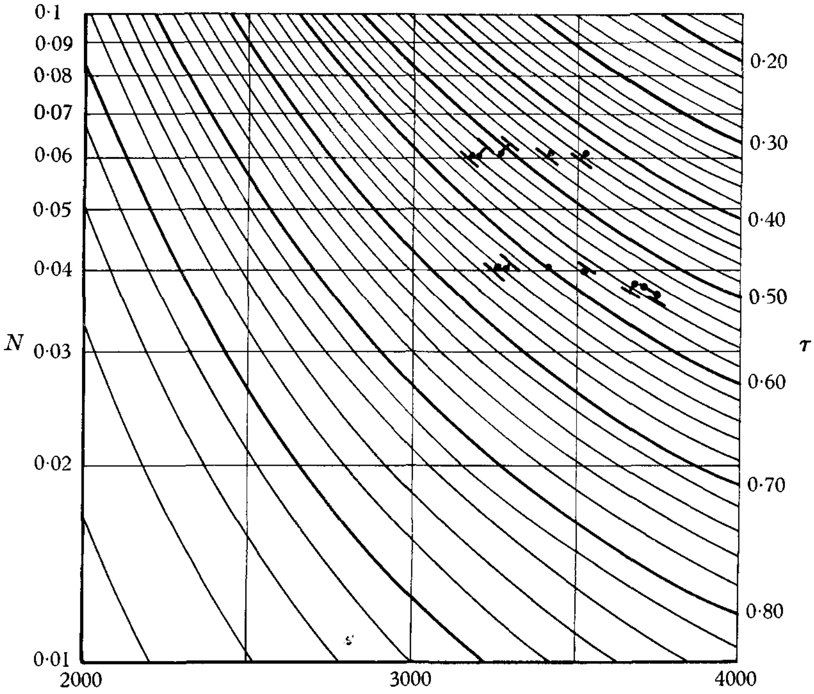

FIGURE 17. Transmission as a function of oxygen molecule density N and temperature at a wavelength of 2283 Å with a band pass of 16 Å, and a path length of 4·57 cm.

where $\bar{K}$ is the average absorption coefficient, L is the path length, and N is the dimensionless oxygen molecule density given by

$$N = c(1-\alpha)(\rho/\rho_0)(p_0/76) \tag{27}$$

p_0 being measured in cm of mercury. The absorption coefficient $\bar{K}$, being proportional to the population of the absorbing level, takes the form

$$\bar{K} = \frac{C\exp(-\bar{E}/kT)}{(T/T_0)^{1\cdot58}} \tag{28}$$

in which $(T/T_0)^{1\cdot58}$ is an approximation to the temperature dependence of the partition function. Wurster & Treanor found that $C = 1\cdot30 \times 10^4\,\mathrm{cm}^{-1}$ and $\bar{E} = 1\cdot06 \times 10^4\,\mathrm{cm}^{-1}$ for the band at 2283 Å, with a band width of 16 Å. However, there is a possibility that scattered light was present in these experiments (Wurster 1962) and so several calibrating runs were made to measure the transmission behind shock waves. In these runs the measurements were made upstream of the expansion aerofoils. Assuming the same value of $\bar{E}$, C was found to be $1\cdot32 \times 10^4\,\mathrm{cm}^{-1}$. Transmissions calculated with this value of C are plotted in figure 17 as a function of oxygen molecule density and temperature. Also plotted are the experimental transmissions, represented by a line parallel to the lines of constant transmission, and connected by a short line to a point giving the temperature and density of the run as determined by the Mach number.

Since the absorption measurement effectively measures the population of some vibrational level of the gas, it only determines the gas temperature and density if the gas is in vibrational equilibrium. Using Widom's (1957) fit to Blackman's (1956) measurements of the oxygen vibrational-relaxation time, the vibrational-relaxation time behind the expansion was found to be less than 5 μsec for the present experiments. This was considered sufficiently smaller than the time at which the measurement was made (about 40 μsec after leaving the expansion) for the gas to have attained vibrational equilibrium.

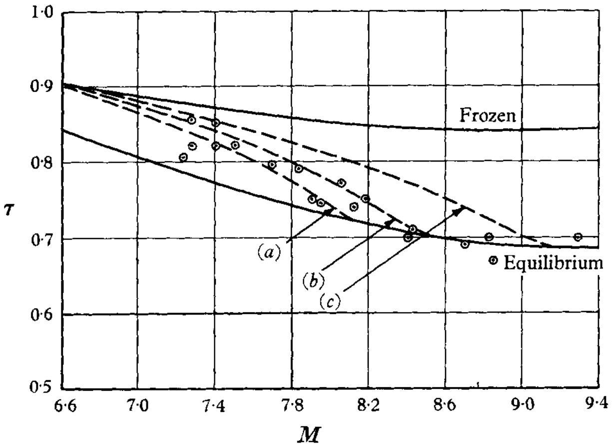

FIGURE 18. Transmission *vs* shock Mach number. The dashed lines are calculated assuming a value of the recombination rate constant. (*a*) $k^{O_2} = (3 \times 10^{18}/T)$ c.c.^{2}/mole^2 sec, (*b*) $k^{O_2} = (2 \times 10^{18}/T)$ c.c.^{2}/mole^2 sec, (*c*) $k^{O_2} = (10^{18}/T)$ c.c.^{2}/mole^2 sec.

6. Experimental results

The experimental values of transmission 11 cm downstream of the expansion for a $c = 0{\cdot}30$ mixture of oxygen in argon are plotted against shock Mach number in figure 18. Also shown are theoretical values of transmission for various assumed rate constants. To calculate these curves the rate equation

$$q\frac{d[\mathrm{O_2}]}{dx} = \frac{d[\mathrm{O_2}]}{dt} = \Sigma_{\mathrm{M}}\, k_R^{\mathrm{M}}[\mathrm{O}]^2\,[\mathrm{M}] - \Sigma_{\mathrm{M}}\, k_D^{\mathrm{M}}[\mathrm{O_2}]\,[\mathrm{M}], \tag{29}$$

in which k^{M} represents a rate constant with M as the third body, was integrated under the following assumptions: (1) constant density during recombination; (2) constant rate constant; (3) dissociation terms negligible. The first assumption was shown to be a good approximation by the ideal-dissociating gas calculations; the second is valid if the recombination process involves a small temperature change; and the third assumption holds unless the reaction has proceeded almost to equilibrium. Integration yields

$$k_R^{\mathrm{O_2}} = \frac{q_2}{4(c\rho_2/m)^2\, x[1+(k^{\mathrm{A}}/k^{\mathrm{O_2}})\,(1-c/c)]}\left[\frac{1}{\alpha} + P(\log\alpha - \log\{1+P\alpha\})\right]_{\alpha_1}^{\alpha}, \tag{30}$$

where
$$P = \left(2\frac{k^{\mathrm{O}}}{k^{\mathrm{O}_2}} - 1\right) \Big/ \left\{1 + \frac{k^{\mathrm{A}}}{k^{\mathrm{O}_2}}\left(\frac{1-c}{c}\right)\right\}.$$

Dissociation rate studies have shown that the rate constant with argon as third body is about an order of magnitude smaller than that with oxygen molecules as third body, and consequently, $k^{\mathrm{A}}/k^{\mathrm{O}_2}$ was taken as 0·1. In an attempt to evaluate the rate constants due to oxygen molecules as third body and oxygen atoms as third body, runs were made at $c = 0{\cdot}42$ and $c = 0{\cdot}30$. However, the runs at $c = 0{\cdot}42$ showed that recombination had proceeded to equilibrium at all Mach numbers between 7·5 and 9·5. It was therefore necessary to assume a value of $k^{\mathrm{O}}/k^{\mathrm{O}_2}$; following Rink *et al.* (1961), the value of 3 was used. With these values of the ratios of the rate constants, equation (30) was used to calculate the degree of dissociation 11 cm downstream of the expansion for three assumed values of the rate constant k^{O_2}. With α known, the density and temperature can be calculated from the real gas equivalents of equations (19) and (20), and hence the transmission can be determined from figure 17. The state of the gas behind the expansion was calculated in a manner analogous to that described for the ideal dissociating gas, although the exact shock equations and the real gas enthalpy were used (see Wilson 1962).

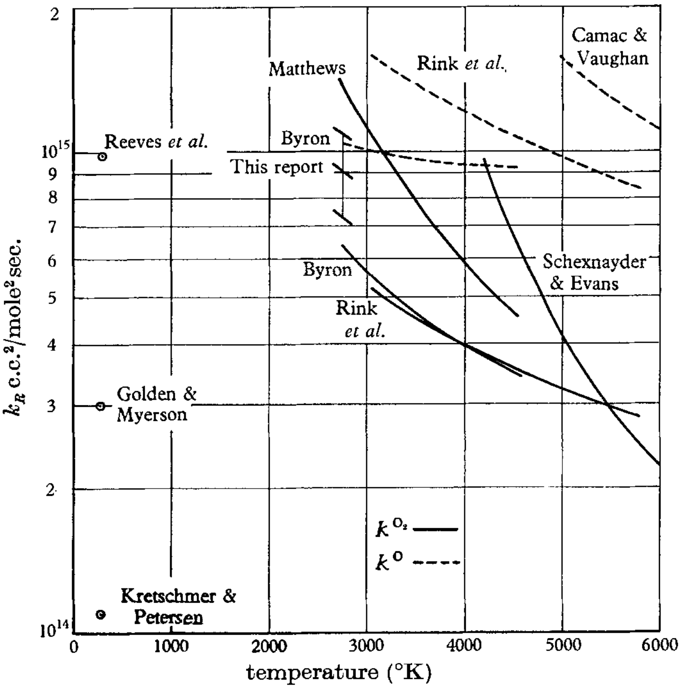

FIGURE 19. Recombination rate constants *vs* temperature.

From figure 18 the recombination rate constant was taken to be

$$k_R^{\mathrm{O}_2} = (2{\cdot}5 \pm 0{\cdot}5 \times 10^{18})\,T^{-1}\ \text{c.c.}^2/\text{mole}^2\,\text{sec.} \qquad (31)$$

Although the recombination rate constant is expressed here as having an inverse temperature dependence, this was not verified by the experiment, the temperature range being too low.

Conclusions

In figure 19 recombination rate constants obtained from dissociation rate measurements by dividing the dissociation rate constant by the equilibrium constant are plotted as a function of temperature, and can be compared with the present direct measurement. It will be seen that the value obtained here lies below that found by Matthews, but above that of Byron and the extrapolated value of Rink and co-workers. Thus, the direct measurement of the recombination rate constant can be said to be in reasonable agreement with the values obtained from dissociation rate studies. Since in this experiment equilibrium is approached in the opposite sense, i.e. from an excess of atoms instead of from a deficit, this agreement justifies the use of the relation $k_D/k_R = K$ in non-equilibrium situations.

The author is grateful to Professor E. L. Resler, Jr. for suggesting this research, and for invaluable guidance during its course. The author would also like to express appreciation to Dr S. R. Byron for many helpful discussions.

This work was largely supported by the Mechanics Branch of the Office of Naval Research under contract Nonr. 401 (25).

REFERENCES

Anderson, O. L. 1961 *United Aircraft Corp. Rep.* R-1828-1.

Blackman, V. 1956 *J. Fluid Mech.* **1**, 61.

Byron, S. R. 1959 *J. Chem. Phys.* **30**, 1380.

Camac, M. & Vaughan, A. 1961 *Avco-Everett Research Lab. Research Rep.* 84 (AFBMD-TR-60-22).

Ferri, A. 1961 *Fundamental Data obtained from Shock-tube Experiments.* London: Pergamon Press.

Freeman, N. C. 1957 *AGARD Rep.* no. 133.

Golden, J. A. & Myerson, A. L. 1958 *J. Chem. Phys.* (*Letters to the Editor*), **28**, 978.

Kretschmer, C. B. & Petersen, H. L. 1960 *J. Chem. Phys.* **33**, 948.

Lighthill, M. J. 1955 *Higher Approximations* in *General Theory of High Speed Aerodynamics.* Oxford University Press.

Lighthill, M. J. 1957 *J. Fluid Mech.* **2**, 1.

Matthews, D. L. 1959 *Phys. Fluids*, **2**, 170.

Reeves, R. R., Manella, G. & Harteck, P. 1960 *J. Chem. Phys.* **32**, 632.

Rink, J. P., Knight, H. T. & Duff, R. E. 1961 *J. Chem. Phys.* **34**, 1942.

Schexnayder, C. J. & Evans, J. S. 1961 *N.A.S.A. TR R*-108.

Widom, B. 1957 *J. Chem. Phys.* **28**, 940.

Wilson, J. 1962*a* A measurement of the recombination rate of oxygen. Paper presented at AGARD specialists' meeting on 'The high temperature aspects of hypersonic flow', Brussels. To be published by Pergamon Press, London.

Wilson, J. 1962*b* A shock tube measurement of the recombination rate of oxygen. *Ph.D. thesis.* Cornell University, Ithaca, N.Y.

Wurster, W. H. 1962 Private communication.

Wurster, W. H. & Treanor, C. E. 1959 *Cornell Aero. Lab. Rep.* no. AD-1118-A-10.

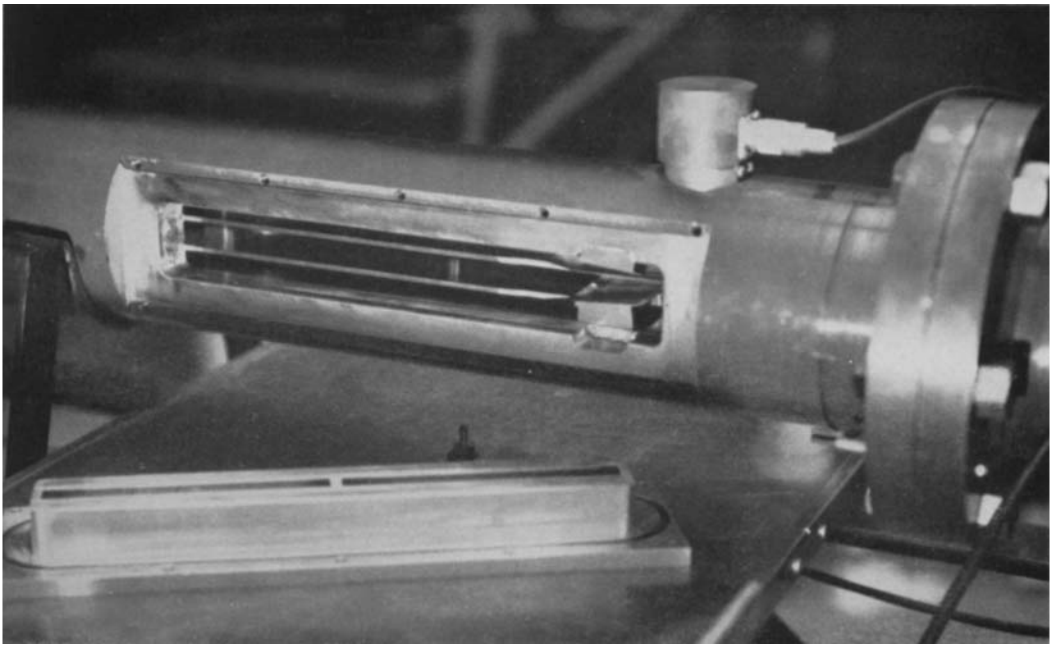

FIGURE 1 (plate 1). Photograph of test section showing expansion aerofoils and constant-area channel.

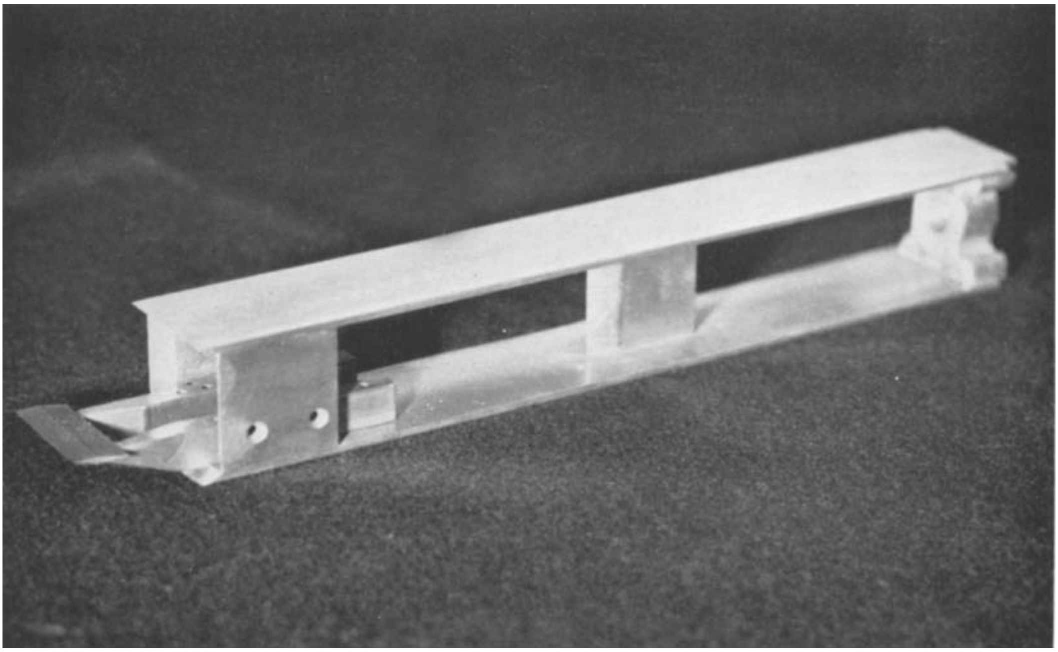

FIGURE 11 (plate 1). Model used in density measurement.

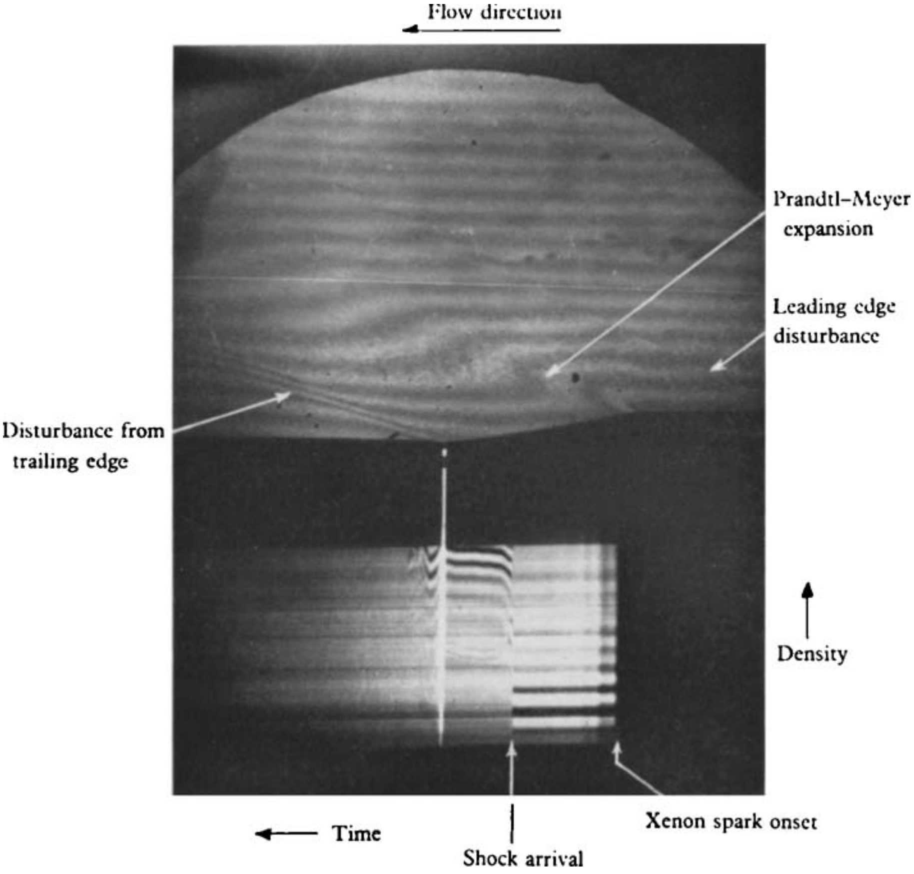

FIGURE 12 (plate 2). Interferogram of flow over the model.

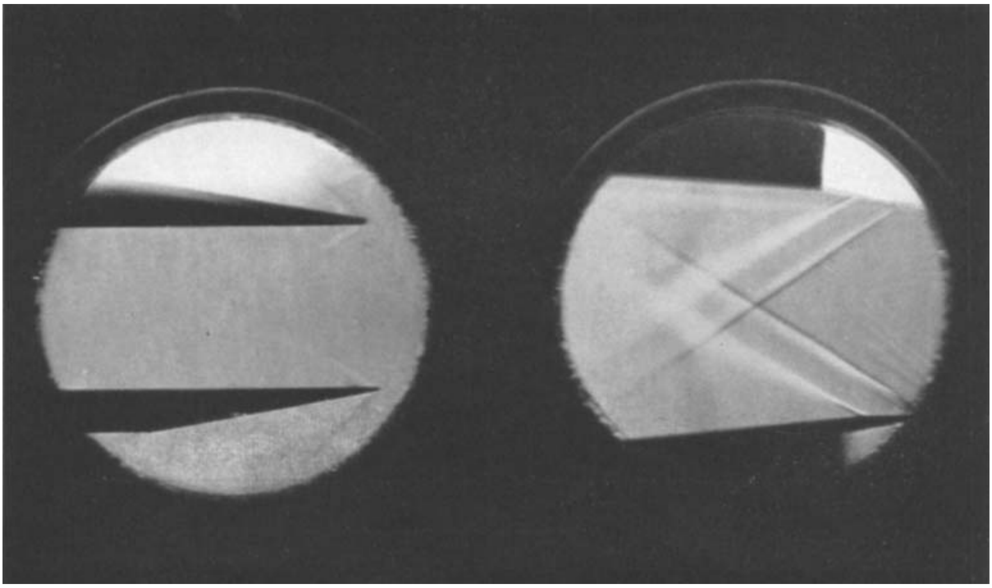

FIGURE 14 (plate 2). Schlieren picture of flow in test section.